

A New Image-Based Real-Time Flame Detection Method Using Color Analysis

Wen-Bing Horng, Jian-Wen Peng, and Chih-Yuan Chen

Abstract—A new image-based real-time flame detection method is proposed in this paper. First, fire flame features based on the HSI color model are extracted by analyzing 70 flame images. Then, based on these flame features, regions with fire-like colors are roughly separated from an image. Besides segmenting fire flame regions, background objects with similar fire colors or caused by color shift resulted from the reflection of fire flames are also separated from the image. In order to get rid of these spurious fire-like regions, the image difference method and the invented color masking technique are applied. Finally, a simple method is devised to estimate the burning degree of fire flames so that users could be informed with a proper warning alarm. The proposed method is tested with seven diverse fire flame video clips on a Pentium II 350 processor with 128 MB RAM at the process speed of thirty frames per second. The experimental results are quite encouraging. The proposed method can achieve more than 96.97% detection rate on average. In addition, the system can correctly recognize fire flames within one second on the initial combustion from the test video clips, which seems very promising.

Index Terms—Color analysis, color masking, burning degree estimation, flame detection.

I. INTRODUCTION

FIRE flame detection is a very important issue because it is closely related to every people's safety and property. Today, most frequently used flame detection techniques are usually based on particle sampling, temperature sampling, and air transparency testing, in addition to the traditional ultraviolet and infrared flame detectors [1]. However, most of these detectors suffer from some severe problems. They require a close proximity to the flame. In addition, they are not always reliable, because they do not always detect the combustion itself. Instead, they detect the byproducts of combustion, which may be produced in other ways. Therefore, they usually result in higher false rates. Furthermore, all of these methods seldom provide additional descriptive information about flame location, size, burning degree, and so on.

Recently many research works on visual fire flame detection are proposed. This is because images can provide more reliable information. Healey et al. [2] presented a fire detection system using color video input for a pre-allocated view on some ideal

conditions. Noda and Ueda [5] used gray-scale images obtained from infrared cameras to detect fire in tunnels. Yamagishi and Yamaguchi [7] also proposed a fire flame detection algorithm for color images based on the HSV color space and artificial neural networks. Foo [3] presented methods for detecting fire in aircraft dry bays and engine compartments from gray-scale images. All of the above methods require a stationary camera. In addition, most of them are designed for a specific environment. Very recently, Phillips et al. [6] proposed a sophisticated method for recognizing flames in color video. However, their method does not consider the temporal variation of flames. Besides, the approach is too complicated to process in real-time.

In order to have an image-based flame detection monitoring system to be of practical use so that users would be informed with a fire alarm as early as possible and they could view the flame images on displays, the system must work in real-time and must be applied to more general environments instead of being restricted on some specific situations. In this paper, a new visual real-time flame detection method is proposed based on machine vision techniques and the theory of chromatics to meet the above requirements. The intuitive HSI color model is chosen to describe flame features extracted from a set of flame images. The color separation method is applied to roughly segment regions with fire-like colors based on the extracted flame features. Then, the image difference method and the invented color masking technique based on chromatics are used to remove spurious fire-like regions, such as objects with similar fire colors or areas reflected from fire flames. Finally, the burning degree of fire flames is estimated to give users a proper warning alarm. The proposed method is tested with seven diverse fire flame video clips on a Pentium II 350 processor with 128 MB RAM. The experimental results show that the proposed method can achieve approximately 97% detection rate on average with thirty frames per second. In addition, the method can recognize fire flames within one second from the test videos, which seems very promising.

The rest of the paper is organized as follows. Section 2 gives a brief description of the HSI color model. Section 3 builds a fire flame feature model. Section 4 presents the proposed flame detection method. Section 5 shows the experimental results. Finally, the paper concludes in the last section.

II. PRELIMINARIES

Let N be the set of natural numbers, (x, y) be the spatial coordinates of a digital image, and $M = \{0, 1, \dots, l-1\}$ be a set of positive integers representing intensities of each R , G , and B

W.-B. Horng, J.-W. Peng, and C.-Y. Chen are with the Department of Computer Science and Information Engineering, Tamkang University, Taipei, Taiwan 25137, ROC (e-mail: horng@mail.tku.edu.tw, pchw8598@mail.hrps.tp.edu.tw, 891190117@s91.tku.edu.tw).

component in the RGB color model. Then, a *color image* function can be defined as the mapping $f: N^2 \rightarrow M^3$.

The *color* of a pixel with coordinates (x, y) , denoted as $f(x, y)$, is a triple (r, g, b) , where r, g , and b are the intensities of the R, G , and B components, respectively. The origin, $(0, 0)$, is at the upper-left corner of an image with the x -axis horizontal and the y -axis vertical.

The three components of the HSI color model [4] are *hue* (H), *saturation* (S), and *intensity* (I , or brightness). Hue represents a dominant (pure) color as perceived by an observer. Saturation refers to the amount of white light mixed with a hue. Two important facts make the HSI color model useful to simulate the color sensing properties of the human visual system. First, the intensity component is decoupled from the color information in an image. Second, the hue and saturation components are intimately related to the way in which human beings perceive color.

The detailed conversion from the familiar RGB color model to the HSI color model can be found in [4]. In the following, the formulas for conversion are briefly listed for reference.

$$i = \frac{1}{3}(r + g + b) \quad (1)$$

$$s = 1 - \frac{3}{(r + g + b)} [\min(r, g, b)] \quad (2)$$

$$h = \begin{cases} \theta & \text{if } b \leq g \\ 360 - \theta & \text{if } b > g \end{cases} \quad (3)$$

$$\theta = \cos^{-1} \left\{ \frac{\frac{1}{2}[(r-g) + (r-b)]}{[(r-g)^2 + (r-b)(g-b)]^{1/2}} \right\} \quad (4)$$

In the above equations, the values of r, g , and b of the RGB model are normalized in the range $[0, 1]$. For convenience of discussion and image processing, the hue, saturation, and intensity components of the HSI model are normalized into the ranges: $0^\circ \leq h \leq 360^\circ$, $0 \leq s \leq 100$, and $0 \leq i \leq 255$.

III. BUILDING A FLAME FEATURE MODEL

According to the commonsense knowledge, it is known that fire flames usually display reddish colors, emit light and heat, and change shapes rapidly. It is also known that the colors of flames become blue when the fire temperature is high, and become red to yellow when the temperature is low. In the study of image-based flame detection, it is necessary to build a more precise *flame feature model* for vision-based fire detection systems.

In this research, 70 flame images are used to analyze the color features of fire flames according to the HSI color model. The adoption of the HSI color model is because it is intimately related to the way in which human beings perceive colors, as described previously. According to the empirical analysis from the set of flame images, the hue values for fire flames from red to yellow are usually in the range $[0^\circ, 60^\circ]$. As to the blue fire flames of higher temperatures, the hue values fall into the range $[200^\circ, 280^\circ]$.

It seems more complicated for analyzing the saturation and

intensity of fire flames. However, it can be divided into two cases to consider. For brighter environments (i.e., larger combustion areas relative to the entire image), fire burns more violently. In this case, the saturation values are distributed in the range $[40, 100]$, and the intensity values are in the range $[127, 255]$. On the other hand, for darker environments (i.e., smaller combustion areas relative to the image), fire burns more peacefully. In this case, the saturation values are in the range $[20, 100]$, and the intensity values are in the range $[100, 255]$. The empirical analysis results for the fire flames with colors from red to yellow are summarized in Table I.

TABLE I
FEATURES OF FIRE FLAMES

Environment	Hue	Saturation	Intensity
Brighter	$0^\circ \sim 60^\circ$	40~100	127~255
Darker	$0^\circ \sim 60^\circ$	20~100	100~255

This research mainly focuses on the detection of the usual lower temperature fire flames, whose color features as listed in the above table. The higher temperature blue fire flames are not considered in this discussion. However, simply changing the detection parameters, such as the hue range, the blue fire flames could be still recognized.

IV. THE PROPOSED FLAME DETECTION METHOD

The proposed fire flame detection method can be divided into three major phases: (1) segmentation using color separation, (2) removal of spurious fire-like regions, and (3) estimation of the burning degree of fire flames, as depicted in Fig. 1. In the first phase, based on the visual features of the fire flame model, fire-like color areas are roughly separated from an input image frame. Then, in the second phase, spurious regions caused by fire reflection or with similar fire-like colors are removed by the image difference and the color masking techniques. Finally, the burning degree of fire flames is roughly estimated in the last phase to provide users a proper fire alarm. The following subsections will elaborate on each of these phases in detail.

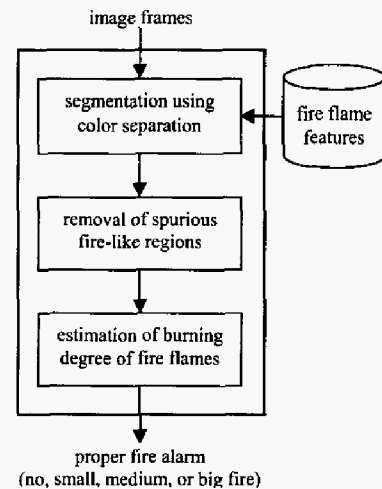


Fig. 1. The flow chart of the proposed flame detection method.

A. Segmentation Using Color Separation

A *color set*, C , is a set of colors such that for each color in the set, represented as a triple (h, s, i) in the HSI color model, the following conditions are satisfied: $h_1 \leq h \leq h_2$, $s_1 \leq s \leq s_2$, and $i_1 \leq i \leq i_2$, in which $[h_1, h_2]$ is the range of hue, $[s_1, s_2]$ is the range of saturation, and $[i_1, i_2]$ is the range of intensity of the color set C . Formally, the color set may be denoted as:

$$C([h_1, h_2], [s_1, s_2], [i_1, i_2]) = \{(h, s, i) \mid h_1 \leq h \leq h_2, s_1 \leq s \leq s_2, \text{ and } i_1 \leq i \leq i_2\}. \quad (5)$$

The extracted fire flame features in the previous section will be used as the basis for defining color sets of fire flames. The color separation algorithm for an input image, $f(x, y)$, based on some fire flame color set, C_f , is as follows: For each pixel in the image, if the color of the pixel does not belong to the color set, then set the pixel color to black (a background color, denoted by *black*); otherwise, keep the pixel color unchanged. The result image, $g(x, y)$, after performing the above color separation can be represented as:

$$g(x, y) = \begin{cases} \text{black}, & \text{if } f(x, y) \notin C_f \\ f(x, y), & \text{otherwise} \end{cases} \quad (6)$$

As illustrated in Fig. 2, the fire areas are almost completely extracted. Notice that some other areas with fire-like colors caused by the reflection of fire flames are also extracted.

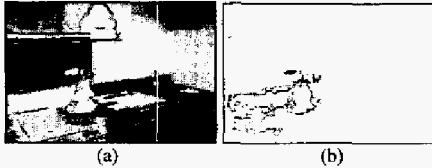


Fig. 2. (a) Fire image; (b) Color separation (white background color for easily viewing).

B. Removal of Spurious Fire-like Regions

After performing color separation on a flame image, only the colors belong to the color set of flame features are remained; others are set to the background color. However, two situations need to be considered.

- 1) Due to the reflection of the fire flames, some objects will change its appearance colors (hues) as well as its brightness to be similar to those of fire flames. Such a phenomenon is called *color shift*, as illustrated by the wall of the kitchen in Fig. 2(a).
- 2) Non-fire objects with similar fire-colors will be mistaken as fire flames and thus are extracted.

For the first situation, Fig. 3(a) shows another case of color shift, in which smoke fills up the entire image. After performing color separation, many non-fire areas are kept due to the smoke changing its color resulted from the reflection of fire flames, as shown in Fig. 3(b). After performing image difference, many non-fire regions still exist, as illustrated in Fig.

3(c). This may be all right for fire detection. If the fire source needs to be more precisely located, the remaining non-fire regions should be removed as completely as possible. By carefully examining the color shift problem, it is found that since the fire color of the smoke is resulted from the reflection of fire source, its intensity and saturation must be lower than the fire source. Thus, if the lower intensity and lower saturation colors are removed further, the result image can keep only the fire information, as shown in Fig. 3(d).

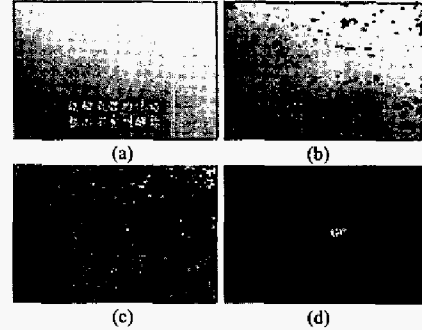


Fig. 3. (a) A fire image with smoke; (b) Result after performing color separation; (c) Result after performing image difference; (d) Result after removing lower intensity and lower saturation colors.

For the second situation, if the color of a background object is similar to that of fire flames, then the image difference method, a technique usually used in object tracking, might be used to remove such an object. Suppose that $g_i(x, y)$ and $g_j(x, y)$ are two images after performing color separation as before. The result of image difference, $h(x, y)$, can be represented as:

$$h(x, y) = |g_i(x, y) - g_j(x, y)| = \begin{cases} |r(g_i(x, y)) - r(g_j(x, y))| \\ |g(g_i(x, y)) - g(g_j(x, y))| \\ |b(g_i(x, y)) - b(g_j(x, y))| \end{cases} \quad (7)$$

where $|\cdot|$ is the absolute function, and $r(\cdot)$, $g(\cdot)$, and $b(\cdot)$ are the functions to extract the red, green, and blue color components of an image, respectively. That is, the difference of two colors takes their absolute values of the red, green, and blue components. And the result of image difference is obtained by computing the difference of every pair of pixel colors.

However, for color images, simply performing color subtraction will encounter some problems. For example, the difference of two reddish colors will result in dark cyan color, as shown in Fig. 4. One way to cope with this problem is to perform color separation again on the result of color difference. Figs. 5(a) and 5(b) are two consecutive flame images after performing color separation. Fig. 5(c) is the result of image difference of the above two images. Notice that the odd green color regions appear in the lower half of Fig. 5(c). Fig. 5(d) is the result after performing color separation again on Fig. 5(c). Notice also that the overlap regions of fire areas in consecutive images disappear. That is, some fire areas are lost.

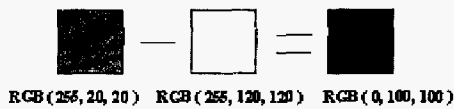


Fig. 4. Color difference of two reddish colors resulting in a dark cyan color.

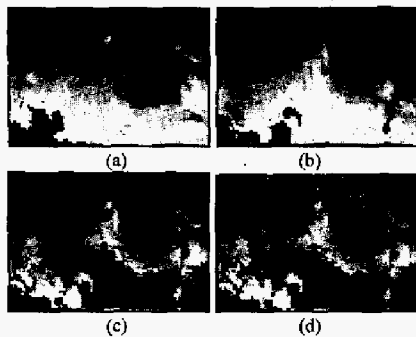


Fig. 5. (a) and (b) Two consecutive fire images after color separation; (c) Result of image difference; (d) Result after performing color separation again.

One special situation occurs when the color shift phenomena happens too fast so that the reflective color at the same place of two consecutive images differs quite a lot. After performing color separation and image difference, the resulting image still contains some apparent fire-color residues in the non-flame regions. In this case, some theory of chromatics can be applied to solve such a problem.

Fig. 6 shows a hue cycle from chromatics consisting of saturated colors. When performing color separation to extract fire flame colors from the hue cycle with hue in the range $[0^\circ, 60^\circ]$, the R value will be approximately 255, the G and the B values will be somewhere in the range $[0, 255]$ (suppose that the intensity of each of the primary colors is in the range $[0, 255]$). When two fire colors in the hue cycle subtract each other, the R value will be near zero, and the G and the B values will be in the range $[0, 255]$, which falls in the colors ranging from green to cyan to blue. This is the reason why, as illustrated in Fig. 4, when two fire colors perform image subtraction, the result color becomes dark cyan.

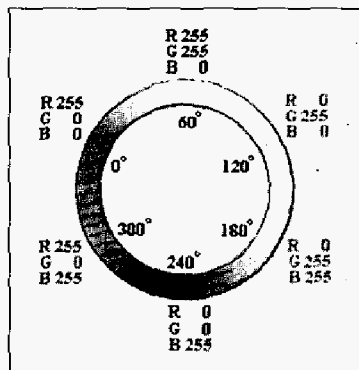


Fig. 6. A hue cycle of chromatics for explaining the odd green colors resulted from image difference of two fire colors.

For convenient discussion, artificial fire images, as shown in

Fig. 7, are created for illustration. Figs. 7(a) and 7(b) are two consecutive fire images after performing color separation, in which background is filled with the black color. Fig. 7(c) is the result of image difference of Figs. 7(a) and 7(b). Due to color shift, suppose that objects numbered 2 and 4 are reflective color of the light source. Object numbered 3 remains in the same region. It will be removed in the image difference step. After performing color separation again, objects numbered 2 and 4 still remain, as shown in Fig. 7(d). This causes the problem of color residue.

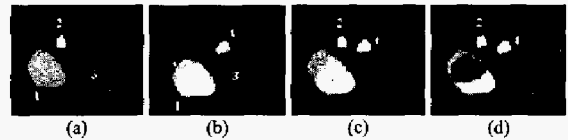


Fig. 7. (a) & (b) Two consecutive, artificial fire images after color separation; (c) Result after image difference of (a) and (b); (d) Result after color separation again.

In order to solve the problem of color residue, a technique from the theory of chromatics may be used to remove the objects numbered 2 and 4 caused by color shift. If the background color is designated by one of the neighbor primary colors in the hue cycle of the fire color, such as blue or green instead of black, then the remained color residues will be correctly removed after performing image difference. In this paper, the blue color is arbitrarily chosen as the background color, as shown in Figs. 8(a) and 8(b). After performing image difference, objects numbered 2 and 4 change their colors outside the range of fire colors, as shown in Fig. 8(c). Therefore, after performing color separation again, objects numbered 2 and 4 are removed in the final image, as shown in Fig. 8(d). The technique of choosing a particular background color to remove spurious regions caused by color shift is called the *color masking*. The chosen background color is called the *mask color*. Notice that in the final result, as shown in Fig. 8(d), the fire flame regions become thinner, like fire flame contours, which will be helpful in estimating the burning degree of fire flames, as discussed in the following.

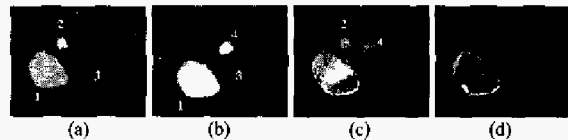


Fig. 8. (a) & (b) Two consecutive, artificial fire images after color separation with blue as the background color; (c) Result after image difference of (a) and (b); (d) Result after color separation again.

By using the mask color, denoted by *mask*, for color masking, Eq. (6) for color separation should be modified as:

$$g'(x, y) = \begin{cases} \text{mask}, & \text{if } f(x, y) \notin C_f \\ f(x, y), & \text{otherwise} \end{cases} \quad (8)$$

And the image difference used in the color masking technique should be modified as:

$$h'(x, y) = |g'_i(x, y) - g'_j(x, y)| \quad (9)$$

The color masking technique can easily remove the color residue after image difference and, thus, is very suitable for tracking the object with specific range of colors. Figs. 9(a) and 9(b) are two consecutive fire images. Fig. 9(c) is the result of image difference using the original color separation method (i.e., Eq. (6)). Notice that many residues around the fireman remain in Fig. 9(c). Fig. 9(d) is the result of using the color masking technique. Here only the fire flame regions are kept.

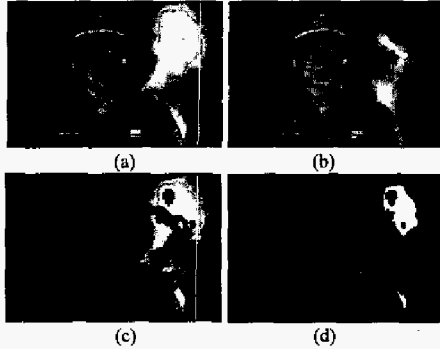


Fig. 9. (a) and (b) Two consecutive fire images; (c) Result after image difference using original color separation on (a) and (b), more color residues of red clothes around the fireman; (d) Applied the color masking and the residues on (c) are removed.

C. Estimation of the Burning Degree of Fire Flames

Up to now, there is little research on estimating the burning degree of fire flames based on visual flame detection. In this paper, a simple method is proposed for roughly estimating the burning degree of flames.

After performing color masking, the result image, $h'(x, y)$, keeps the fire flame boundaries, which resemble to the contours of the flames. When the combustion is getting more violent, flame contours change their shapes more rapidly. Therefore, the variation of flame contours might be used to estimate the burning degree of fire flames.

Since only the contour information is needed, the corresponding binary image, $b(x, y)$, of a contour image, $h'(x, y)$, is defined as follows:

$$b(x, y) = \begin{cases} \text{black,} & \text{if } h'(x, y) = \text{black} \\ \text{white,} & \text{otherwise} \end{cases} \quad (10)$$

That is, in the contour image, set all remaining fire colors to white (denoted as *white*), and the result image is called a *binary contour image*. The difference, $d(x, y)$, of two binary contour images, $b_i(x, y)$ and $b_j(x, y)$, can be represented as:

$$d(x, y) = |b_i(x, y) - b_j(x, y)| = \begin{cases} \text{black,} & \text{if } b_i(x, y) = b_j(x, y) \\ \text{white,} & \text{otherwise} \end{cases} \quad (11)$$

The difference image, $d(x, y)$, is called a *contour difference*

image. Since the image difference used in this research takes the absolute values of differences, in effect, the result will be the same as performing the exclusive-or (XOR) operation on two binary images.

Fig. 10 illustrates the whole process to obtain the final binary contour images. Figs. 10(a)–(c) are three consecutive fire images with interval equal to two frames. The corresponding results after performing modified color separation using a mask color on the above three images are shown in Figs. 10(d)–(f). Fig. 10(g) is the result after performing image difference on Figs. 10(d) and 10(e) and performing color separation again. Similar operations are performed on Figs. 10(f) and 10(g) to obtain Fig. 10(h). Finally, Fig. 10(i) is the result contour difference image of Figs. 10(g) and 10(h).

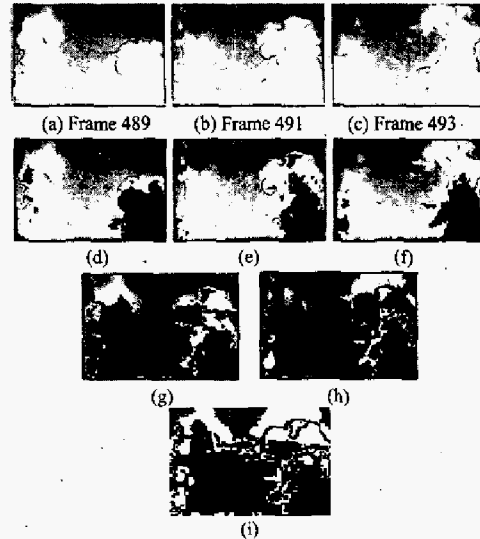


Fig. 10. (a)–(c) Three consecutive fire frames with frame number labeled; (d)–(f) Results after performing modified color separation with color masking on (a)–(c); (g) Result after performing color masking and color separation on (d) and (e); (h) Result after performing image difference and color separation on (e) and (f); (i) Result contour difference image of (g) and (h).

After obtaining a contour difference image, the number of white pixels on it could be used as a measure of the burning degree of fire flames. Define the *white pixel ratio*, r_w , of a contour difference image, $d(x, y)$, to be

$$r_w = \frac{n_w}{n}, \quad (12)$$

where n_w is the number of white pixels, and n is the total number of pixels in the image $d(x, y)$. The higher the white pixel ratio is, the more violently the fire flames burn. Because the area projected to the image plane varies due to different distances, it is impossible to define absolute values to estimate the burning degrees of flames. Small detected fire flame areas may be big fire captured from far distance. Conversely, large recognized fire flame regions may be small fire captured from near distance. In order to alleviate this problem, a small fraction

(for example, 0.03), s , is given by users according to the situation of the input video. Two threshold values, t_1 and t_2 , are defined such that $t_i = i \times s$, for $i = 1$ and 2. These threshold values serve as references for estimating the burning degree of fire flames. In this research, three estimated different burning degrees as used, in addition to no fire. They are "small", "medium", and "big". If the white pixel ratio r_w is equal to 0, no fire is detected. If $0 < r_w \leq t_1$, it is assumed that small fire is recognized. Similarly, if $t_1 < r_w \leq t_2$, medium fire is assumed. Finally, if $r_w > t_2$, the system recognizes it as big fire. As shown in Fig. 11, four alert signs (i.e., green, yellow, orange, and red) are designed to indicate the different burning degree of fire flames. The green sign stands for no fire. The yellow, orange, and red signs represent small, medium, and big fire, respectively.

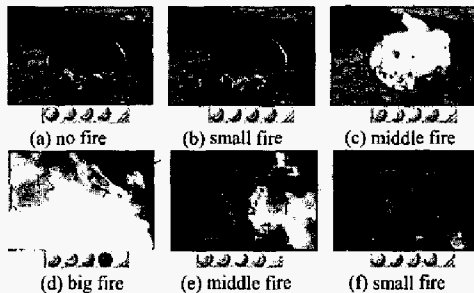


Fig. 11. Four alert signs indicating different burning degrees of fire flames (green: no fire, yellow: small, orange: medium, red: big).

V. EXPERIMENTAL RESULTS

The proposed flame detection method is tested with seven fire video clips for a variety of conditions, including daytime and nighttime, indoor and outdoor. The experimental results of the proposed flame detection method are shown in Table II. The field n_f is the number of frames of a video clip. The field n_i is the number of frames containing fire flames in the video. The field f_- is the number of false negative flames, which means that the system does not detect fire flames in an image frame while there are indeed fire frames in it. Similarly, the field f_+ is the number of false positive flames, which means that the system recognizes fire flames in an image frame while there are no fire flames at all. The *detection rate*, r_d , of a video is defined as the ratio

$$r_d = \frac{n_c}{n_f}, \quad (13)$$

where n_c is the number of correctly detected frames (including fire and non-fire frames) in a video clip.

The system can process the input video of thirty frames per second on a Pentium II 350 processor with 128 MB RAM in real-time. The average detection rate can achieve more than 96.94%. Especially, in video 1 (the worst case) the number of false negative frames is 24, which implies that the system can detect fire within one second because the processing speed is 30 frames per second. The reason of false negative detection is

due to very small fire flames on the initial combustion, as shown in Fig. 12(a). Notice that, even for the nearly steady flames such as spirit lamps of videos 2 and 7, the system can still detect lamp flames correctly, as illustrated in Figs. 12(b) and 12(c). In general, the experimental results are very encouraging and promising.

TABLE II
EXPERIMENTAL RESULTS OF FIRE FLAME DETECTION

video	n_f	n_i	f_-	f_+	r_d (%)	Description
1	674	575	24	0	96.44	Fire and fireman
2	790	755	0	1	99.87	Spirit lamp in the daytime
3	317	267	0	25	92.11	Explosion
4	55	2	0	1	98.18	Gun fire
5	1189	875	0	45	96.22	Fire in kitchen
6	250	117	11	0	95.60	Fire with smoke
7	520	471	0	9	98.27	Spirit lamp in the nighttime
total	3795	3062	35	81	96.94	

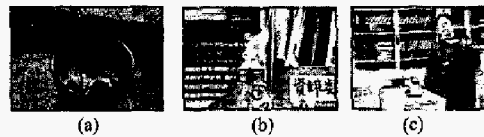


Fig. 12. (a) False negative detection on the initial combustion; (b) Spirit lamp with complex background; (c) Spirit lamp near a girl with red clothes.

VI. CONCLUSION

In this paper a new image-based real-time flame detection method is proposed. It is based on the computer vision techniques and some theory of chromatics. Several new ideas are presented in this new flame detection method. The color masking technique is proposed to cope with the color residue problem. In addition, a simple method is devised to estimate the burning degree of fire flames. On a Pentium 350 processor with 128 MB RAM, the method is tested with seven diverse video clips at thirty frames per second. The experimental results show that the method can achieve approximately 97% detection rate. In addition, the system can recognize fire flames within one second on the initial combustion.

REFERENCES

- [1] B. C. Arrue, A. Ollero, and J. R. Martinez de Dios, "An intelligent system for false alarm reduction in infrared forest-fire detection," *IEEE Intelligent Systems*, vol. 15, no. 3, pp. 64–73, May/June 2000.
- [2] G. Healey, D. Slater, T. Lin, B. Drda, A.D. Goedeke, "A system for real-time fire detection," in *Proc. Conf. Computer Vision and Pattern Recognition*, 1994, pp. 605–606.
- [3] S. Y. Foo, "A machine vision approach to detect and categorize hydrocarbon fires in aircraft dry bays and engine compartments," *IEEE Trans. Industry Applications*, vol. 36, pp. 549–466, March/April 2000.
- [4] R. C. Gonzales and R. E. Woods, *Digital Image Processing*, 2nd ed., Prentice-Hall, 2002, ch. 6.
- [5] S. Noda, K. Ueda, "Fire detection in tunnels using an image processing method," in *Proc. Conf. Vehicle Navigation and Information System*, 1994, pp. 57–62.
- [6] W. Phillips III, M. Shah, and N. da Vitoria Lobo, "Flame recognition in video," in *Proc. Fifth Workshop on Applications of Computer Vision*, 2000, pp. 224–229.
- [7] H. Yamagishi and J. Yamaguchi, "Fire flame detection algorithm using a color camera," in *Proc. Int. Symp. Micromechatronics and Human Science*, 1999, pp. 255–260.